UNIVERSITY OF MINNESOTA
ST. ANTHONY FALLS HYDRAULIC LABORATORY

Project Report No. 70

A Water Tunnel Air Content Meter

by
JOHN M. KILLEN
and
JOHN F. RIPKEN

Prepared for
DAVID TAYLOR MODEL BASIN
Department of the Navy
Washington, D.C.
under
Bureau of Ships General Hydromechanics Research Program
S-R009-01-01
Office of Naval Research Contract Nonr 710(42)

February 1964
Minneapolis, Minnesota

PREFACE

A need has existed for some time in cavitation research for a means of measuring size and concentration of minute air bubbles in the ambient waters of hydraulic machinery subject to cavitation.

This problem is particularly acute with regard to the test water of a water tunnel where modelling of a cavitation phenomena is necessary.

Studies of an air content measuring system were carried out at the St. Anthony Falls Hydraulic Laboratory during the period from October 1962 to February 1964, under the sponsorship of the David Taylor Model Basin, Contract Nonr 710(42).

The authors are indebted to Scott D. Christ and John A. Almo for their assistance in the execution of the program.

A B S T R A C T

This paper describes a system for measuring the size and concentration of free air bubble nuclei in the limited ranges of size and concentration thought to exist in a water tunnel.

The system is based on measuring the amplitude attenuation of an acoustic pulse of sound as it is propagated across a water tunnel test section. An arbitrary method is proposed for converting the measured sound attenuation into size and concentration of air bubbles.

C O N T E N T S

LIST OF ILLUSTRATIONS

A WATER TUNNEL AIR CONTENT METER

I. INTRODUCTION

The phenomena of cavitation in water is strongly dependent upon the existing regions of structural weakness in the fluid. These regions are commonly called nuclei and are generally assumed to be small air bubbles which have stabilized at some finite size. Strasberg [1]* indicates that such bubbles in water are probably of the order of 3×10^{-4} cm, in radius.

The mechanism of this bubble stabilization process is at present only vaguely understood. Three theories which in part explain the phenomena are: (a) air entrapment in solid boundary cracks or in suspended particles, (b) organic skin on the air bubbles which inhibits diffusion of gas, and (c) minute solid particles collecting on the bubble wall which take part of the pressure loading and reduce the liquid wall area. Experimental investigations have not yet validated any of these theories.

It may be assumed that all modelled cavitation tests, particularly those involving cavitation inception, will be strongly influenced by the number and size of the air bubble nuclei present in the test water.

It is postulated that the probability of cavitation depends on the probability of a nuclei being swept into a region of flow where the dynamic pressure is sufficient to produce sudden vaporous expansion. The critical low pressure must depend on the size of the bubble and its gas content. The severity of cavitation must depend on the number of nuclei present in a unit volume of the fluid. Since nuclei size and concentration are at present usually unknown, true modelling of cavitation is difficult and inception point experiments are generally not meaningful.

Relationships have been proposed [2] for scale effects in inception studies but these depend on knowledge of the bubble size and concentration. It appears that scaling of cavitation inception conditions will remain obscure pending development of adequate means to measure nuclei.

---

*Numbers in brackets refer to List of References on page 11.

Current methods of measuring the influence of gas content in water tunnel studies usually involve a direct measurement of the total gas (dissolved gas plus free gas) [3, 4]. However, it has been shown by tests at the St. Anthony Falls Hydraulic Laboratory [5, 6] that while total gas or the degree of saturation is an important factor in establishing the free gas or nuclei, it is not the only factor. Under dynamic tunnel conditions many other factors influence the formation and growth of nuclei of the critical size. Furthermore, these tests have shown that free gas values are frequently transient in character and that measurement of nuclei must take place in the test section and must be rapid and continuous in nature if nuclei data are to be correlated with other variables in a tunnel test.

The importance of free air bubbles in cavitation, as evidenced from the references cited, and the difficulty of describing both size and concentration from indirect methods has served as a stimulus for the present effort to measure both size and concentration of the free gas bubbles in a water tunnel test section.

Of the various methods available for the measurement of an air bubble suspension the most promising seem to be either acoustical or optical [7]. The acoustical was chosen as offering the highest sensitivity and better averaging over a volume.

Previous efforts to relate the sonic characteristics with the liquid-gas characteristics of a bubble mixture may be found in Ref. [1, 5, 8, 9, 10].

II. BUBBLE SIZE MEASUREMENTS

The measurement of bubble size in a water tunnel experiment seems generally easy to accomplish.

The procedure previously reported [6] consisted of exciting the gasified flowing water in a tunnel test section with a random noise and plotting the noise pressure spectrum as received by a hydrophone mounted in the test section. The noise source and hydrophone are physically separated to require transmission via the test water. A block diagram of the apparatus is shown in Fig. 1 with a typical record from the Panoramic analyzer shown in

Fig. 2. In a non-gasified water, a record of the type shown in Fig. 2 would indicate virtually no attenuation across the entire frequency spectrum depicted. In the presence of free gas, the record as shown in Fig. 2 will be depressed in those frequency bands which approximate the resonant frequency of the free gas bubbles which are present. The relative magnitude of this graphical depression is a measure of the acoustic attenuation and is in turn a measure of the concentration or numbers of bubbles present.

The bubble size is related to the frequency of sound attenuation by the following equation [11]:

$$R_o = \frac{1}{2\pi f_o}\sqrt{\frac{3\gamma P_o}{\rho_2}}\left(\frac{g}{a}\right) \tag{1}$$

where R_o = bubble radius

f_o = resonant frequency of the bubble

γ = ratio of specific heats

P_o = static pressure

ρ_2 = density of the water

$\frac{g}{a}$ = a function arising from heat conduction and surface tension which is plotted as a function of static pressure and frequency in Fig. 3 and is defined in Ref. [11, 12] by the following equation:

$$\left(\frac{g}{a}\right) = \frac{1}{a} + \frac{2\sigma\omega_o}{\sqrt{\frac{3\gamma P_o}{\rho_2}^3}}\left(\frac{1}{a} - \frac{1}{3\gamma}\right)$$

where $\omega_o = 2\pi f_o$

σ = surface tension of water

a = a function plotted in Ref. [11 and 12]

Preliminary measurements on gasified water in the St. Anthony Falls water tunnel test section have shown a frequency attenuation range of approximately 20 to 70 KC at a pressure of 5.2 psia and a temperature of 60 degrees

fahrenheit. This gives a rough bubble size range of 0.0028 to 0.0098 cm radius (0.0022 to 0.0077 inch diameter). The tests referred to above are limited and should not be regarded as necessarily representative of either the St. Anthony Falls water tunnel or water tunnels in general. They are used here as a guide in instrument design as they seem to be the only data available.

The size range quoted above corresponds to the size range which has been observed in a number of unrelated forms of bubble generators and bubble studies, and will not be accepted until more detailed experimental data is available.

If an attenuation pattern on the oscilloscope of the analyzer (i.e. Fig. 2) is observed as gasification progressively increases in the water tunnel, attenuation appears first in the 20 to 70 KC size range and then increases in magnitude and moves to lower frequencies. The bubbles in this size range are evidently not the very small stabilized nuclei, previously referred to in the introduction, which would produce attenuation at a much higher frequency.

The presence of stabilized nuclei would seemingly require a gradual attenuation beginning at frequencies higher than 70 KC and with a progression toward lower frequencies as the bubbles grow. The fact that these higher frequency attenuations are not observed in the tunnel test section suggests that this phase of bubble growth occurs elsewhere in the tunnel circuit. The intense shear vortex actions in and downstream of the pump appear a likely locale for this phase of growth, although such pump action will be considerably modified by the presence of a resorber in the circuit.

It is evident that the bubble size measurement as performed by the methods described here are not defining the basic nuclei which are postulated to exist in undisturbed waters, but are instead defining the bubble product of dynamic tunnel processes. It is these latter large size bubbles which account for the relative ease with which cavitation may be generated in a well gassed tunnel water.

III. CONCENTRATION MEASUREMENTS

Total Concentration by Velocity Propagation

Bubble size measurements alone can have considerable value in applied tunnel operations; however, the sizes would be much more meaningful if associated with a concentration measurement. Possibly the most effective measurement up to the present time has been a total concentration measurement. Total concentration measurement has been successfully accomplished [6] by utilizing the velocity of propagation of an acoustic pulse [5]. The technique involved is as follows:

The change in acoustic velocity as a function of gas concentration is given as

$$\frac{C_x}{C_v} = \sqrt{\frac{P_a}{XE_w + (1 - X)P_a}} \qquad (2)$$

where C_x = velocity of sound in the mixture
C_v = velocity of sound in water
X = concentration of gas by volume
E_w = elasticity modulus of water
P_a = absolute pressure in the gas

There is sufficient change in velocity of propagation at water tunnel pressure to indicate a change in concentration of one part per million.

In order that the foregoing simple relationship applies, it must be established that the bubble sizes present are smaller than the resonant size corresponding to the frequency of the measuring acoustic signal.

In this study an appropriate measuring signal was generated by repetitively discharging a condenser through the windings of a magnetostrictive transducer resonant at 7.5 KC. A measurement of the delay time of the above pulse as it traversed the distance between the transmitter and receiver gave a value for velocity of propagation which could be applied to the equation to yield a total free gas concentration value.

Although the total free gas value of the water has some use, the most meaningful part of this free gas is that which occurs as larger size

bubbles. In consequence, a more desirable concentration measurement would be one which yields the concentrations for a series of bubble radii intervals. It was to this end that the major effort of the present program was directed.

Concentration by Size Intervals Using Random Noise

The attenuation pattern of a random noise signal as described previously (i.e. Fig. 2) has an attenuation magnitude for discrete bubble sizes in proportion to bubble concentration.

Two difficulties arose with attenuation measurements with such random noise. First, for water in which bubbles were not in evidence, standing waves appeared; standing waves did not appear in the presence of bubbles. In consequence, measurement of acoustic pressure levels at a single hydrophone location could not yield a measure of gas concentration. Second, it was found difficult to generate a sufficiently high random signal noise level to override the inherent noise level of the water tunnel at higher water velocities.

In initial studies the first difficulty was circumvented, at the expense of increased complexity in readout, by moving the transmitter or receiver an incremental distance along the transmission path in the bubbly mixture. With this technique, the data were obtained by recording the random signal received by the hydrophone on one channel of a data tape recorder while another channel recorded the hydrophone position.

Attenuation measurement consisted of measuring the output of the tape recorder at a series of frequencies with a frequency analyzer and plotting amplitude against displacement at each frequency on an x-y plotter. From the slope of the resulting lines, attenuation in db per unit length could be measured at each frequency.

The method of traversing the transducer units to avoid standing wave influence provided acceptable signals at low water tunnel velocities, but was unsatisfactory at high water tunnel velocities because of the high background noise and limited output of the electronic noisemaker. Considerable effort was expended in trying to develop a more powerful yet compact noisemaker utilizing a cavitating fluid. These noisemakers recirculated various fluids (water, oil, mercury) at high speeds through various geometric

housings designed to produce severe cavitation. In these studies useful acoustic pressure levels and spectrum characteristics were achieved in small cavitating venturis. However, a sufficiently reproducible acoustic value could not be consistently obtained and these noise sources were abandoned as a source for attenuation measurement.

The random noise method was deemed inadequate for detailed concentration measurements. However, the circuit of Fig. 1 employing a noise generator is a valuable monitor of tunnel gas content in a qualitative way when used in conjunction with the procedure to be described later and is desirable to retain for that purpose.

Concentration by Size Intervals Using Pulsed Sine Waves

As an alternative, a pulse system was adopted as shown in Fig. 4. A piezoelectric transducer is pulsed for a few cycles of a sine wave at various frequencies between 20 and 100 KC. The decrease in amplitude at a hydrophone a short distance from the transmitter gives a measure of attenuation along the transmitted path.

The measurement procedure adopted is the conventional one. The attenuator is adjusted (Fig. 4) so that the size of the pulse on the oscilloscope screen is the same regardless of the attenuation present. In this way the incremental increase in attenuation can be read directly from the attenuator box.

Figures 5 and 6 show two photographs of the oscilloscope screen for typical water tunnel conditions.

The theory and procedure of conversion of attenuation to concentration is a graphical one, described in Appendices I and II.

Description of Equipment

The equipment used was assembled from available laboratory components.

The interconnection of equipment has been shown in Figs. 1 and 4.

The pulser* used is a non-standard item which was available from earlier work. Its schematic diagram is shown in Fig. 8. This is a modification of the circuit shown in Ref. [13].

The transmitting transducer construction is shown in Figs. 9 and 10. It was constructed by stacking 4 Honeywell type C-11 ceramic transducer elements so that they were excited in parallel. The elements were 3/4-in. in diameter by 1/8-in. thick. The whole assembly was mounted in a lucite block as shown so that it could be inserted in a port in the water tunnel test section. Figures 11 and 12 show the acoustic pressure response and the electrical characteristics along the axis under pulse conditions. The response to random noise is shown in Fig. 2.

The transducer was driven by a Scott amplifier which was used throughout most of the testing. This amplifier is not particularly well suited to the task. A power stage which works quite well has been added recently to the pulser shown in Fig. 8.

The receiving hydrophone was a type LC33 Atlantic Research. This hydrophone is a very convenient shape for mounting in a water tunnel; however, its acoustic area is much too large. A smaller hydrophone would seem desirable to reduce diffraction patterns. It should be possible to develop a small hydrophone along the line suggested in Ref. [13].

Figure 5 establishes zero attenuation for a no-gas condition. Figure 6 shows a typical pattern occurring with 10 db attenuation and a gasified condition.

The sound attenuation by a group of different size bubbles (i.e. Fig. 6) forms the analogue of a band suppression network in the frequency domain. A typical hypothetical response of such a network to a packet of sine waves is sketched in Fig. 7 as it could appear on an oscilloscope screen. When measuring attenuation in a simple way, comparison of amplitudes must be made in regions of the pulse where the change of amplitude between successive cycles is small. This requires a long pulse duration which is difficult to obtain in the short distances and at the low frequencies of this particular application.

---

*General Radio type 1396-A Tone Burst Generator should serve this purpose.

The change in pulse shape is apparent in Figs. 5 and 6. The attenuator under these conditions can only be adjusted to a visual average of the amplitude reduction. However, the large attenuation, which results from small bubble concentrations at the reduced pressures in a water tunnel, lessens the need for a great accuracy in attenuation measurements.

Measurement of attenuation by the pulse system of Fig. 4 at a single frequency point can be accomplished in a few seconds and a sufficient number of observations can be made in a few minutes to outline the necessary bubble spectrum. This is because the range of frequencies in any one test is not expected to exceed 40 to 50 KC.

The preamplifier had a frequency response flat from 5 cycles to at least 500 KC and a gain of 1,000, and, like the pulser, was available as part of the general laboratory stock.

IV. CONCLUSIONS AND RECOMMENDATIONS

The pulsed noise measuring procedure for estimating free air content in a water tunnel fluid as described in this report provides a reasonably rapid method for estimating bubble size and concentration.

The method is currently believed to involve a number of conditions and assumptions peculiar to a water tunnel application. These are:

(a) For sufficient sensitivity the ambient test pressure must be low;

(b) Bubble distribution is continuous across any increment of bubble size;

(c) The pulse technique as employed here requires a compromise between numbers of cycles in the pulse, frequency range, path length, and bandwidth of the region of attenuation;

(d) Bubble sizes occurring must be resonant at frequencies between 20 and 100 KC. The 20 KC limit is imposed by the size of the tunnel. The 100 KC is a limit imposed by the particular transducer employed in these tests. The present state of the art of transducer construction should provide easy extension.

If the conditions tabulated above can be met for a water tunnel, then the proposed method should permit development of a specific instrument for routine water tunnel use. The limited tests described in this report do not constitute such a validation and it is for these reasons that further refinement of the instrument system is not recommended at this time.

In view of the fact that the present concepts of the role of nuclei in cavitation phenomena are largely conjectural and that virtually no reliable data exist, specific instrument development is currently premature.

Since the present form of pulsed noise instrument can provide workable water tunnel data, it is proposed that a series of typical water tunnel cavitating experiments be undertaken. These experiments would serve to demonstrate the validity of the assumptions, the limitations of the instrument system and, most important, would provide some quantitative data on the role of free bubbles in cavitation.

Completion of such a study should provide a firm base for the finalized air content instrument design.

LIST OF REFERENCES

[1] Strasberg, M. The Influence of Air-filled Nuclei on Cavitation Inception, David Taylor Model Basin Report 1078, May 1957.

[2] Oshima, R. Theory of Scale Effect on Cavitation Inception in Axially Symmetric Bodies, Reports of the Institute of High Speed Mechanics Tohoku University, Vol 13, 1961-62, pp. 79-91.

[3] Kanellopoulos, E. V. New Method For Measuring Gas Content of Water, Mech. Engr. Research Lab. Fluid Report 69, East Kilbride, Scotland, 1958.

[4] Fitzpatrick, H. M. and Harklerood. A Meter for Continuous Indication of Dissolved Air in Water, David Taylor Model Basin Report 867, October 1954.

[5] Ripken, J. F., and Olson, R. M. A Study of the Influence of Gas Nuclei on Cavitation Scale Effects, University of Minnesota, St. Anthony Falls Hydraulic Laboratory, Progress Report 58, January 1958.

[6] Ripken, J. F. and Killen, J. M. A Study of the Influence of Gas Nuclei on Scale Effects and Acoustic Noise for Incipient Cavitation in a Water Tunnel, University of Minnesota, St. Anthony Falls Hydraulic Laboratory, Tech. Paper No. 27, Series B, September 1959.

[7] Eisenberg, Phillip. Cavitation Chap. 12, Handbook of Fluid Dynamics, V. L. Streeter Editor, McGraw Hill, 1961.

[8] Richardson, E. G. Detection of Gaseous Nuclei in Liquid Using an Ultrasonic Reverberation Chamber, Mechanical Engineering Research Laboratory, East Kilbride Glasgow, Fluid Mechanic Division Note No. 38.

[9] Turner, W. R. Physics of Microbubbles, Vitro Laboratories Technical Note 01654 01-2, Silver Springs, Maryland, August 1963.

[10] Turner, W. R. Ultrasonic Measurement for Microbubble Research, Vitro Laboratories Technical Note 0654 01-1, Silver Springs, Maryland, July 1963.

[11] Devin, Charles. Survey of Thermal Radiation and Viscous Damping of Pulsating Air Bubbles in Water, David Taylor Model Basin Report 1329, August 1959.

[12] Faran, J. J. Sound Scattering by Solid Cylinders and Spheres, Harvard University, Acoustic Research Lab., TM 22, March 1951.

[13] Neubauer, Werner. Sound Sources and Probes for the Measurement of Pulsed Acoustical Waves in Water, Journal Acoustical Society of America, Vol. 34, No. 3, March 1962, pp. 312-318.

[14] Meyer, E. and Skudrzyk, E. On the Acoustic Properties of Gas Bubble Screens in Water, Translation by Charles Devin, Jr. David Taylor Model Basin Translation 285.

[15] Spitzer, Lyman. Acoustic Properties of Gas Bubbles in A Liquid, Office of Scientific Research and Development, National Defense Research Committee Div. 6, Section 6.1, No. 6.1-Sr20-918, 1943.

F I G U R E S

(1 through 12)

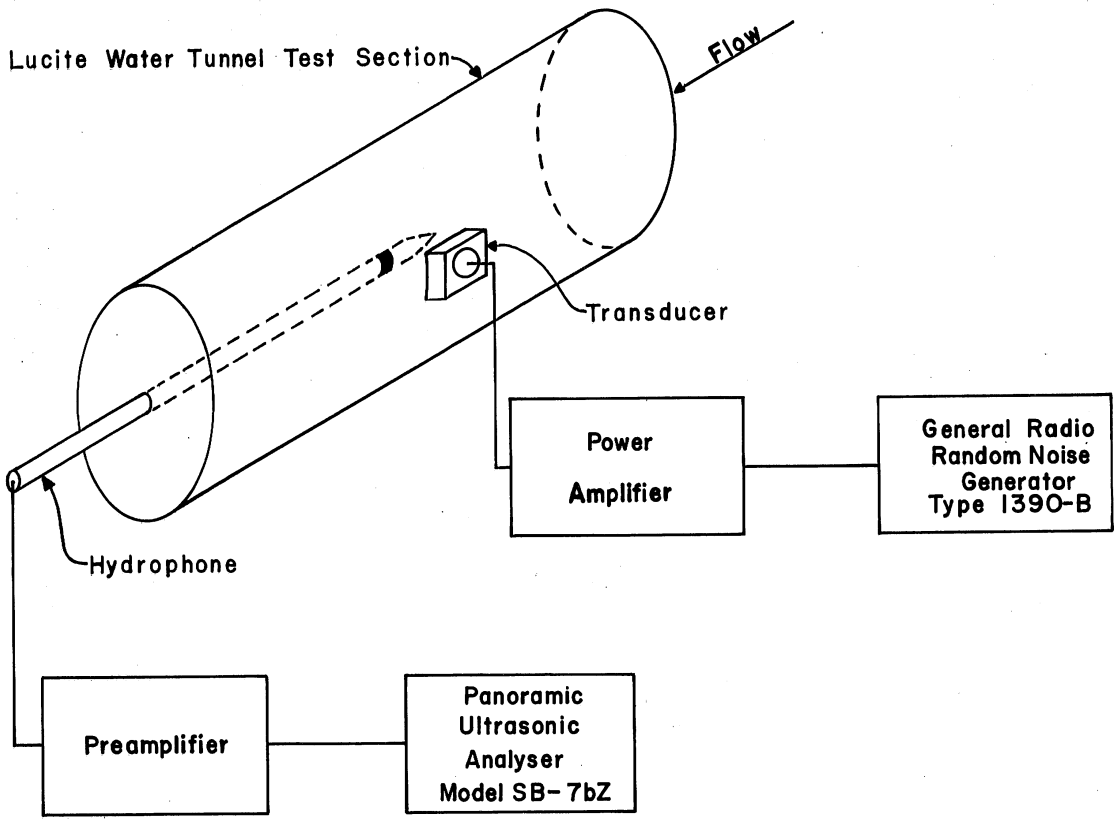

Fig. 1 - Block Diagram of System for Size Measurement with Random Noise

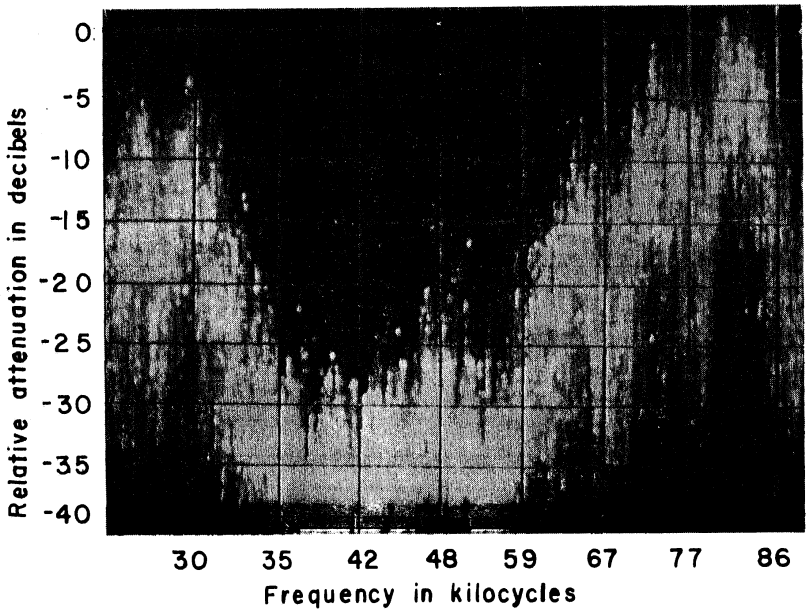

Fig. 2 - Photograph of Oscilloscope Screen Showing Bubble Size Pattern with Random Noise

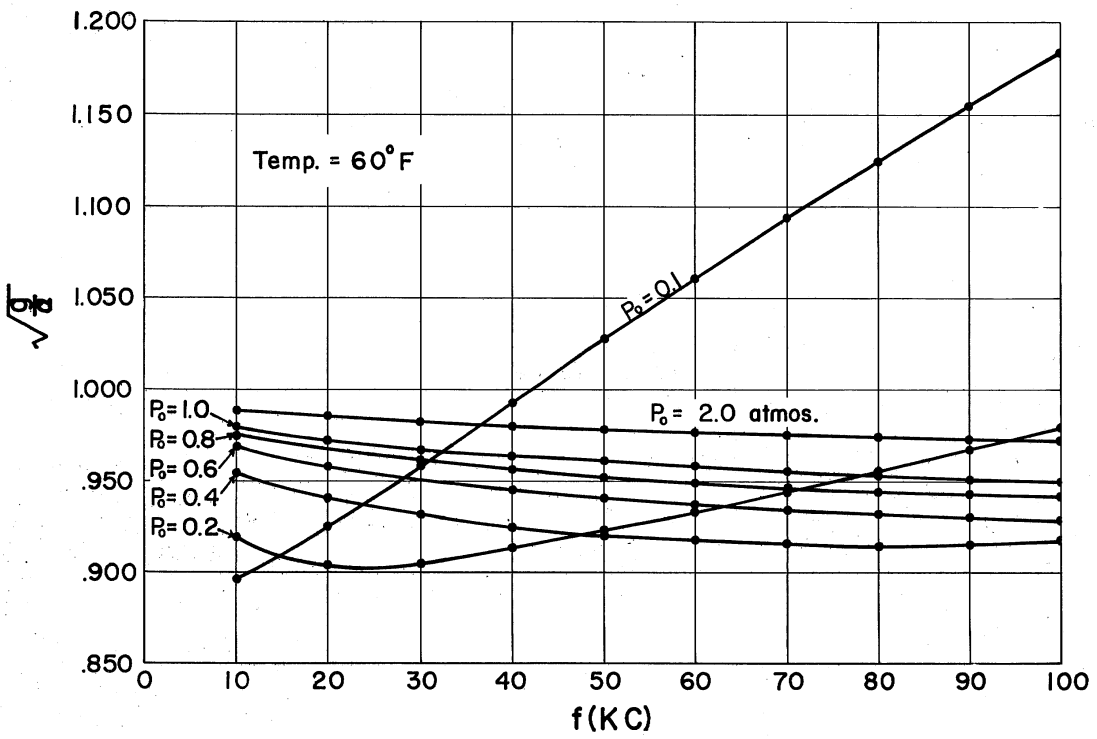

Fig. 3 - Values of $\sqrt{g/a}$

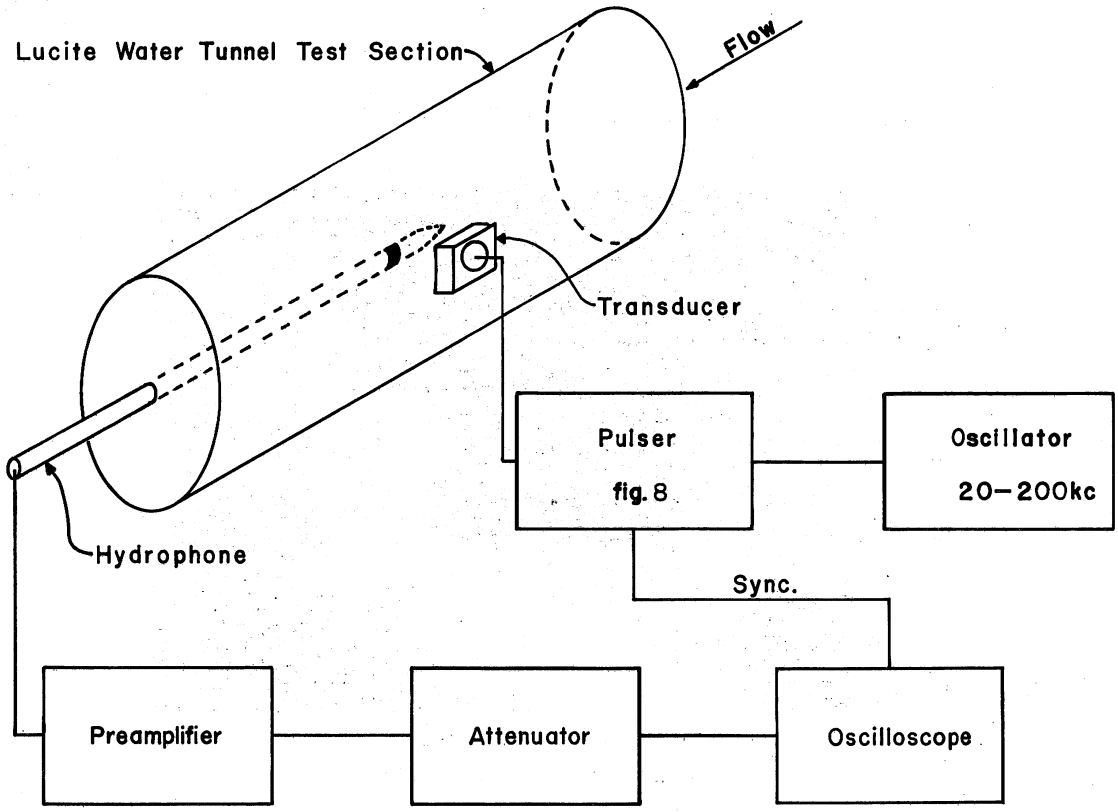

Fig. 4 - Block Diagram of Pulse System for Attenuation Measurement

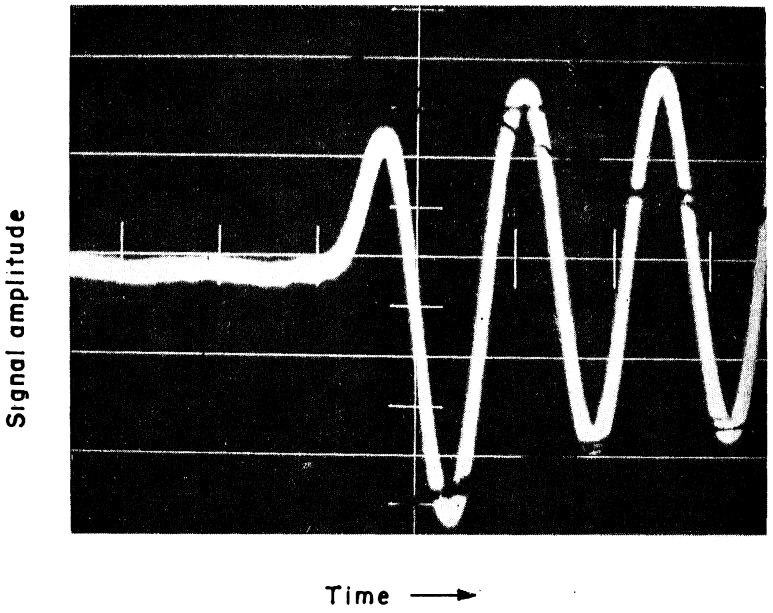

Fig. 5 - Photograph of Sound Pulse in Air Free Water

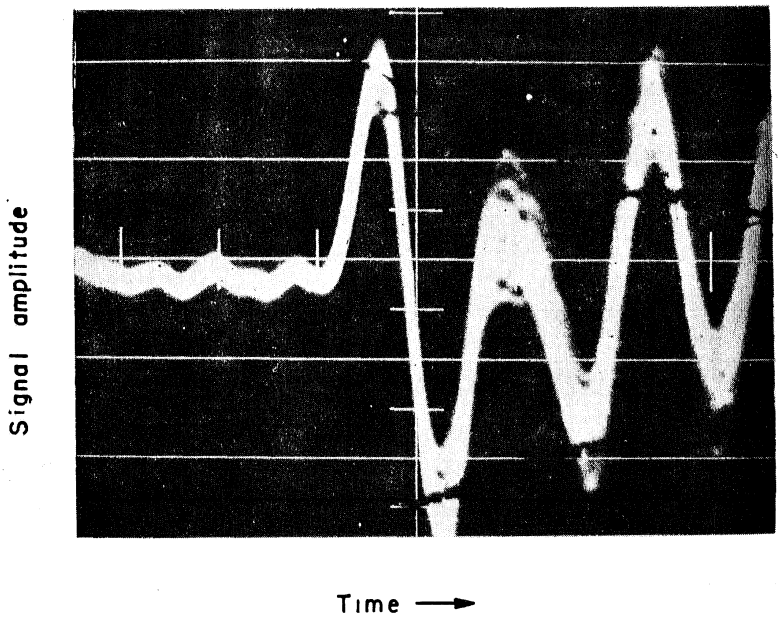

Fig. 6 - Photograph of Sound Pulse as Attenuated by Air Bubbles

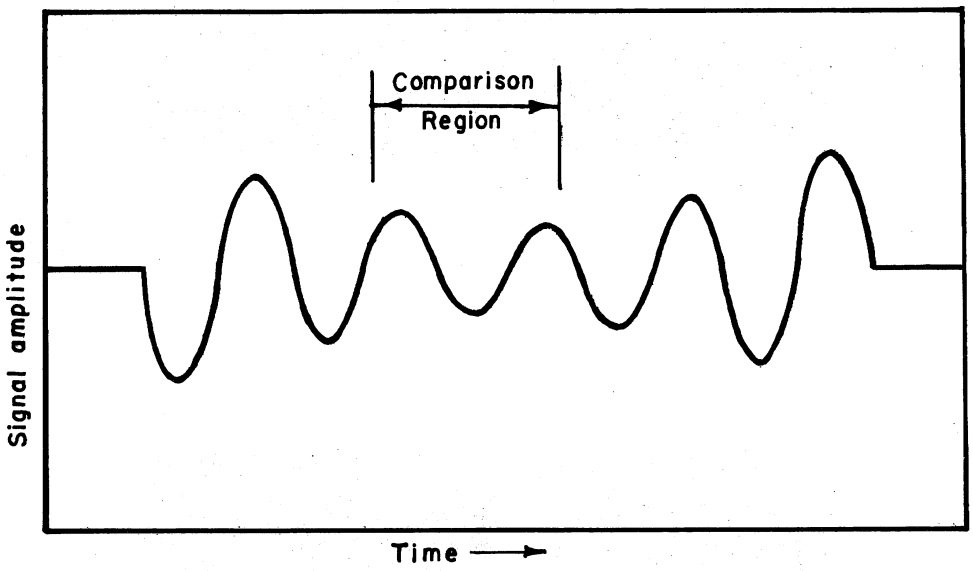

Fig. 7 - Sketch of Pulse Response of a Band Suppression Network at Resonance

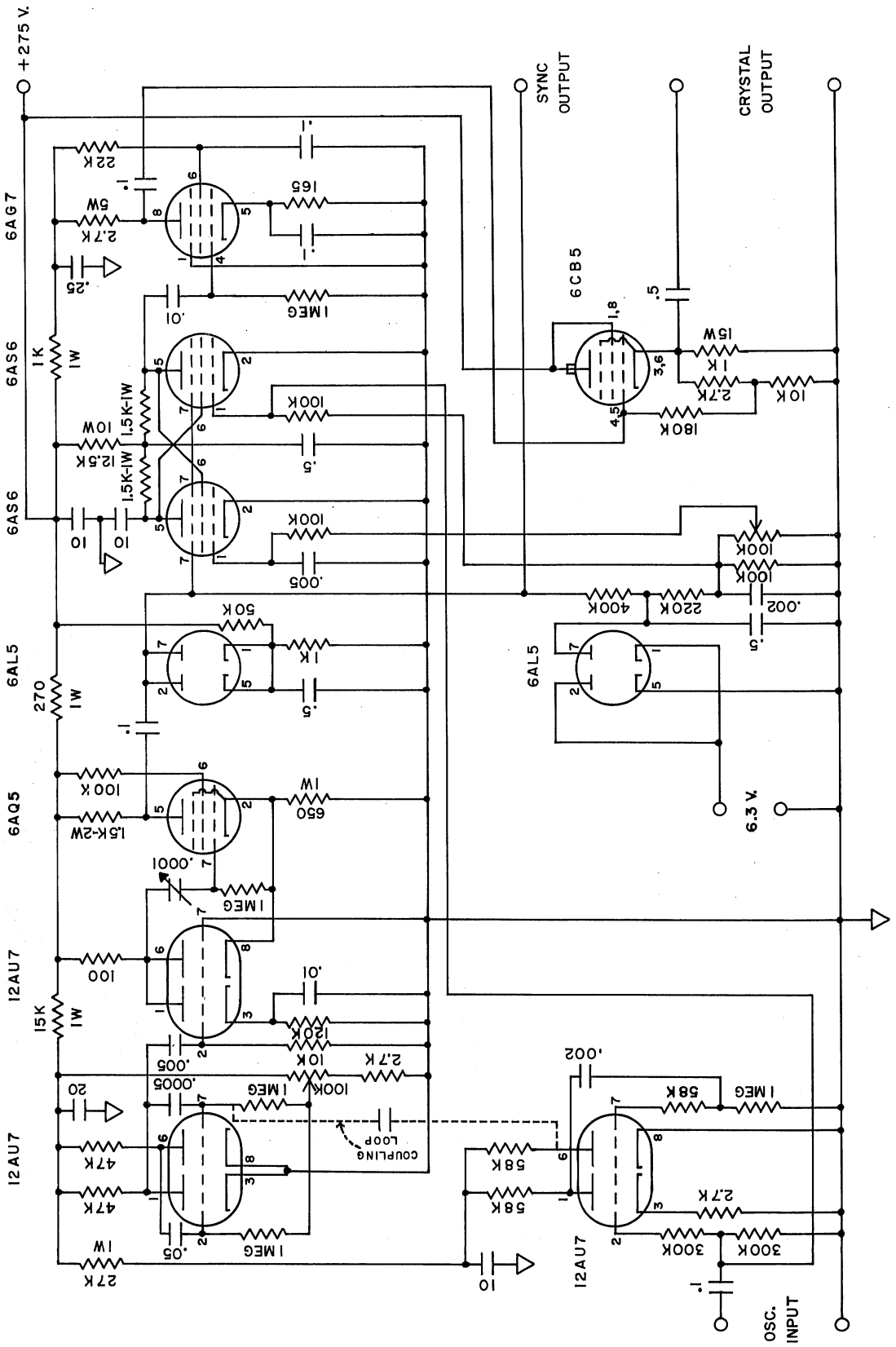

Fig. 8 - Schematic Diagram of Pulser

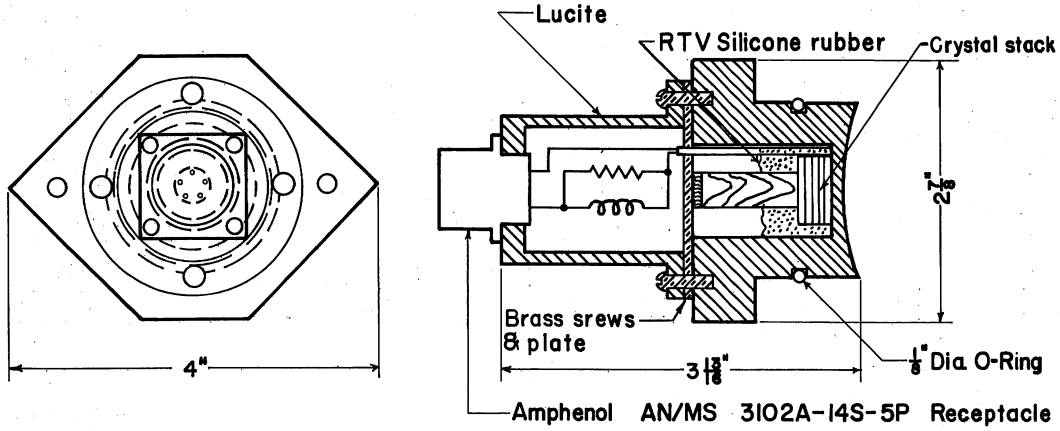

Fig. 9 - Transmitter Construction

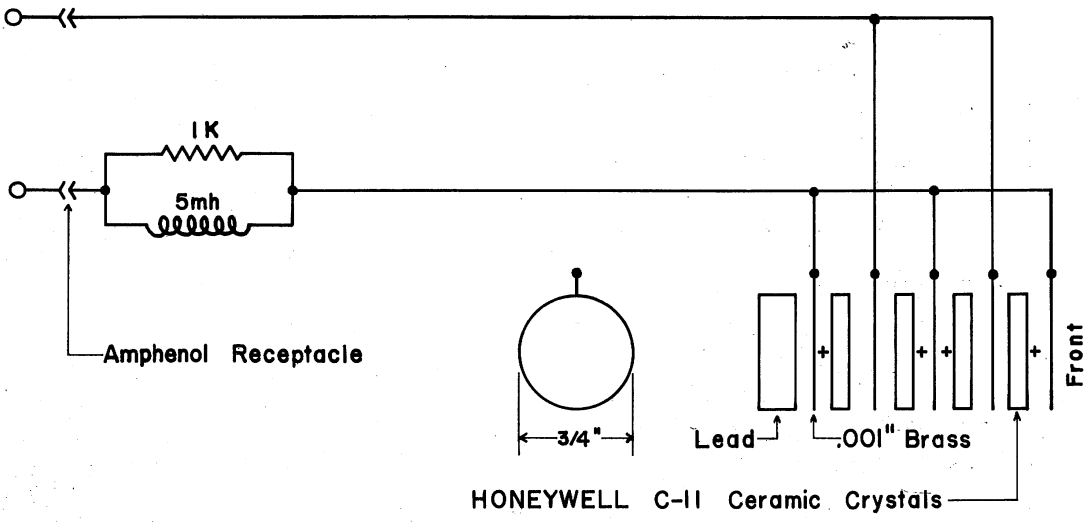

Fig. 10 - Transmitter Element Connectors

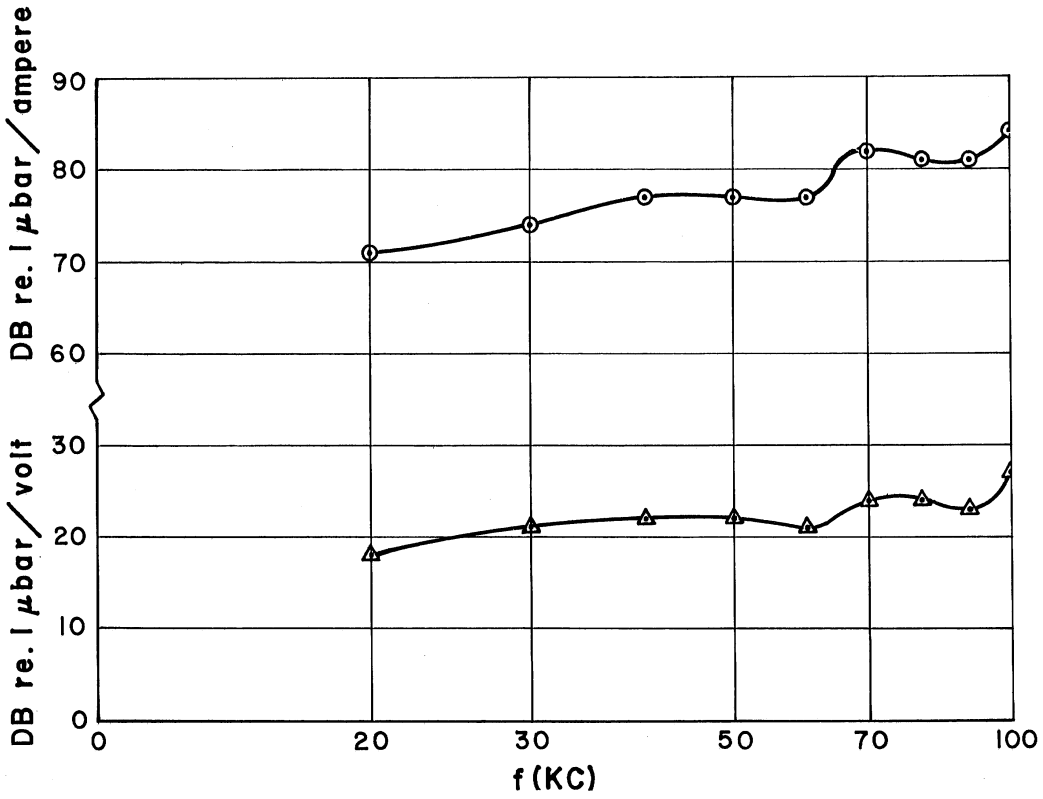

Fig. 11 - Transmitter Response

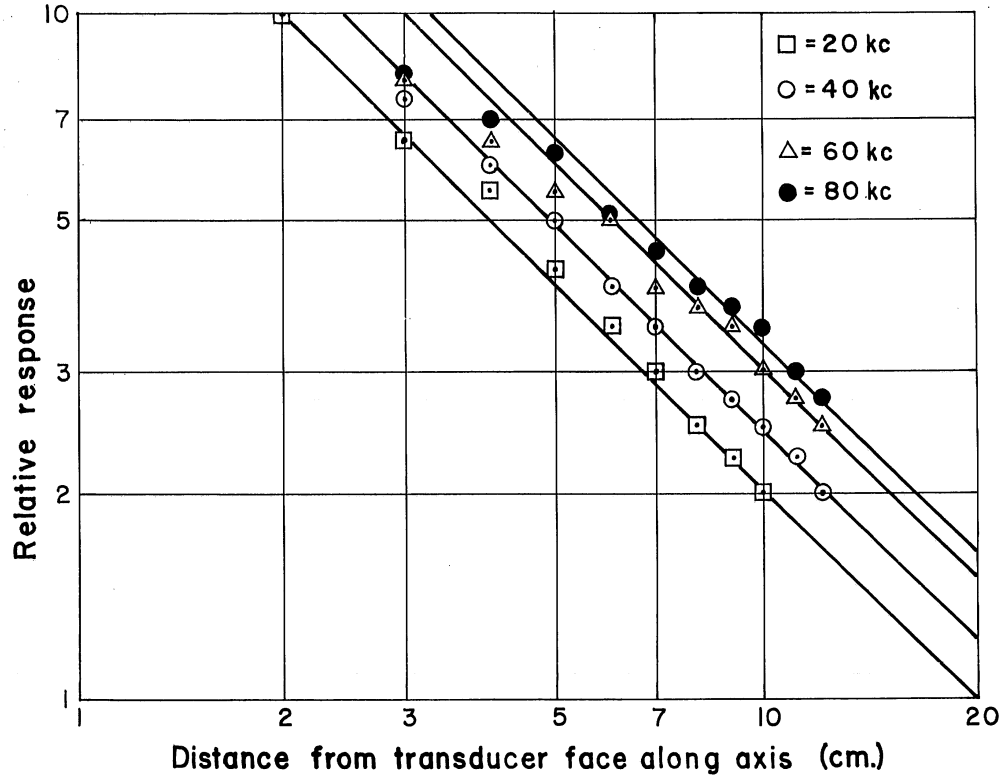

Fig. 12 - Acoustic Pressure Generated on the Axis as a Function of Distance from Face of the Transmitter

A P P E N D I X I

THEORY OF CONCENTRATION MEASUREMENTS

A P P E N D I X I

THEORY OF CONCENTRATION MEASUREMENTS

The measurement of air bubble concentration in water by means of its effect on acoustic attenuation involves the considerations discussed below.

The physical effect which can be measured most readily is the decrease in amplitude of a pressure wave as it propagates through the bubbly mixture.

In bubbly water the reduction in pressure at any point at a distance away from a small transmitter, in the absence of standing waves, can be expressed in terms of an attenuation factor, α, as:

$$P = \frac{P_o}{x} e^{-\alpha x} \qquad (1a)$$

where P_o = pressure at a unit distance from the acoustic center

P = pressure at some point of measurement

x = distance along the acoustic axis of the transmitter from the point where pressure is P_o to the point of measurement

α_1, α_2 = attenuation of water and of a bubbly mixture respectively

If the pressure is measured at a point x in bubble free water, the pressure will be given as $P_1 = \frac{P_o}{x} e^{-\alpha_1 x}$ and in bubbly water at the same point as $P_2 = \frac{P_o}{x} e^{-\alpha_2 x}$. If 20 times the log of the ratio P_1/P_2 is taken then $20 \log P_1/P_2 = 8.68(\alpha_2 - \alpha_1)x$. The increase of attenuation due to the presence of bubbles is then $\alpha x = 20 \log P_2/P_1$ where α is now in decibels per unit length and is the difference, $(\alpha_2 - \alpha_1)$.

The attenuation arising from a number of bubbles, as measured above has been shown [11, 14, 15] to be a function of size, pressure, density, etc. by the following general relationship:

$$\alpha = \int_{r_1}^{r_2} A(r)\tau(r)dr \tag{2a}$$

where $A(r)$ = attenuation function

$\tau(r)$ = concentration function per unit radius

r_1, r_2 = limiting radii of the mixture under consideration

It is $\tau(r)$ which is sought.

Rewriting Eq. (2a),

$$\alpha = \int_{r_1}^{r_2} A(r)\tau_1(r)dr + \int_{r_2}^{r_3} A(r)\tau_2(r)dr \text{ ---} \tag{3a}$$

and assuming an average value of τ_n in each integral, then

$$\alpha \approx \sum_n \tau_n I_n \tag{4a}$$

where $$I_n = \int_{r_n}^{r_{n+1}} A(r)\tau(r)dr$$

Since I_n needs to be evaluated for a relatively small number, (n), of radii intervals the graphical summation of Eq. (4a) becomes relatively easy. An expression for $A(r)$ has been given in Ref. [14] and is reproduced here in its essential elements. This involves the equation of motion for a single bubble of small radius compared to the wave length of the exciting pressure P and can be written

$$M \frac{d^2v}{dt^2} + R \frac{dv}{dt} + Kv = - Pe^{j\omega t} \tag{5a}$$

where M = effective mass of the water surrounding the bubble = $\rho/4\pi r$

R = energy dissipation

K = compressibility of the volume = $\frac{3\gamma P_a}{4\pi r^3}\left(\frac{g}{a}\right)$

v = incremental volume change

ω = 2π times the frequency, f

P_a = ambient pressure

$\frac{g}{a}$ as previously described

The steady state solution for v is known to be:

$$v = \frac{-Pe^{j\omega t}}{\omega^2 M\left[\left(\frac{K}{\omega^2 M} - 1\right) + j\,\frac{R}{\omega M}\right]} \tag{6a}$$

The compressibility of a large number, N, of bubbles of a single size becomes:

$$\bar{K} = \frac{-vN}{Pe^{j\omega t}} = \frac{N}{\omega^2 M\left[\left(\frac{\omega_o^2}{\omega^2} - 1\right) + j\,\frac{R}{\omega_o M}\,\frac{\omega_o}{\omega}\right]} \tag{7a}$$

where $\omega_o = \sqrt{\frac{K}{M}}$ = the resonant frequency

$N = \tau/\frac{4}{3}\pi r^3$

τ = volume concentration

$$\bar{K} = \frac{3\tau Z^2}{\omega_o^2 \rho r^2[Z^2 - 1 + j\eta Z]} \tag{8a}$$

and where $Z = \frac{\omega_o}{\omega}$

$\eta = \frac{R}{\omega_o M}$

$\omega_o^2 r_o^2 = \frac{3\gamma P_a}{\rho}\left(\frac{g}{a}\right)$

ρ = water density

r_o = resonant radius

The velocity of propagation of a wave in a mixture can be written in terms of a complex velocity of propagation $\bar{C}$, Ref. [14].

$$\bar{C} = \frac{1}{\sqrt{\rho \bar{K}}} = \frac{1}{\sqrt{\rho(A - jB)}} \tag{9a}$$

and in turn in terms of a complex compressibility where

$\bar{K} = A - jB$ where A and B are the real and imaginary parts of $\bar{K}$.

The phase velocity

$$C_{ph} = \frac{1}{\text{Real part } (\frac{1}{\bar{C}})} = \sqrt{\frac{2}{\rho A\left[1 + \left(1 + \frac{B^2}{A^2}\right)^{\frac{1}{2}}\right]}} \tag{10a}$$

$$\alpha = \text{Imag. part } \left(\frac{\omega}{\bar{C}}\right) = \frac{\omega}{\sqrt{2}} \sqrt{\rho A} \sqrt{\left(1 + \frac{B^2}{A^2}\right)^{\frac{1}{2}} - 1} \tag{11a}$$

expressing the attenuation α in terms of the phase velocity (C_{ph}) and converting to decibels gives

$$\alpha = \frac{8.68}{\sqrt{2}} \omega \rho C_{ph} B \text{ in decibels/centimeter} \tag{12a}$$

For a mixture of many bubble sizes in which the concentration per cycle is constant and equal to $\tau(r)$ and the damping factor is η the compressibility becomes:

$$\bar{K} = \frac{1}{\rho C_o^2} + \frac{\rho \omega \tau(r)}{2\pi\gamma P_a (\frac{g}{a})} \int_{Z_1}^{Z_2} \frac{Z^2 dZ}{Z^2 - 1 + j\eta Z} = A - jB \tag{13a}$$

where C_o = velocity of propagation of bubble free water

$$A' = \frac{1}{\rho C_o} + \frac{\rho \omega \tau(r)}{2\pi\gamma P_a (\frac{g}{a})} \left[Z + \frac{\eta}{2} \tan^{-1}\left(\frac{\eta Z}{Z^2 - 1}\right) + \right.$$

$$\left. \frac{2 - \eta^2}{2\sqrt{4 - \eta^2}} \frac{\ln}{2} \left(\frac{(2Z - \sqrt{4 - \eta^2}) + \eta^2}{(2Z + \sqrt{4 - \eta^2}) + \eta^2}\right) \right]_{Z_1}^{Z_2} \tag{14a}$$

$$-jB = -\frac{j\rho\omega\,\tau(r)}{2\pi\gamma P_a\left(\frac{g}{a}\right)}\left[\frac{\eta}{4}\ln\left((Z^2-1)^2+\eta^2\right)+\left(\frac{2-\eta^2}{2\sqrt{4-\eta^2}}\right)\left\{\tan^{-1}\left(\frac{\eta}{2Z+\sqrt{4-\eta^2}}\right)-\tan^{-1}\left(\frac{\eta}{2Z+\sqrt{4-\eta^2}}\right)\right\}\right]_{Z_1}^{Z_2} \qquad (15a)$$

In the range of bubble sizes of particular interest the value of η required in Eq. (15a) varies from .05 to 0.1 (see Fig. 1A); consequently, the multiplier on the logarithmic term varies from .0125 to .025 while the multiplier on $\tan^{-1}$ is approximately 1/2. The log term will be neglected for convenience. The term Z is now equal to $\frac{\omega_o - \Delta\omega_o}{\omega}$ and $Z_2 = \frac{\omega_o + \Delta\omega_o}{\omega}$ and ω_o is now a mid value in the interval $Z_2 - Z_1$. The magnitude of B can now be written, neglecting small terms in the denominator, as:

$$B = \frac{\rho\omega\,\tau(r)}{4\pi\gamma P_a\left(\frac{g}{a}\right)}\left[\tan^{-1}\left(\frac{2\eta\left(\frac{2\Delta\omega}{\omega_o}\right)\frac{\omega^2}{\omega_o^2}}{\left(1-\frac{\omega^2}{\omega_o^2}\right)^2+\eta^2\frac{\omega^2}{\omega_o^2}-2\left(\frac{\Delta\omega_o}{\omega_o}\right)^2\left(\frac{\omega^2}{\omega_o^2}\right)\left(\frac{\omega^2}{\omega_o^2}+1\right)}\right)\right] \text{ ---} \qquad (16a)$$

Substituting for $|B|$ in Eq. (12a)

$$\alpha_t = \frac{8.68\,\rho C_{ph}\omega^2\tau(r)}{\sqrt{2}\;4\pi\gamma P_a\left(\frac{g}{a}\right)}\left[\tan^{-1}\left(\frac{2\eta\left(\frac{2\Delta\omega}{\omega_o}\right)\frac{\omega^2}{\omega_o^2}}{\left(1-\frac{\omega^2}{\omega_o^2}\right)^2+\eta^2\frac{\omega^2}{\omega_o^2}-2\left(\frac{\Delta\omega_o}{\omega_o}\right)^2\left(\frac{\omega^2}{\omega_o^2}\right)\left(\frac{\omega^2}{\omega_o^2}+1\right)}\right)\right]$$

$$+ \text{ ---} = \frac{8.68\,\rho C_{ph}\omega^2\tau(r)}{\sqrt{2}\;4\pi\gamma P_a\left(\frac{g}{a}\right)}\left[F\left(\frac{\omega^2}{\omega_o^2}\right)\right] \qquad (17a)$$

This will be the working equation.

If an effort is made to reduce Eq. (17a) to the relationship for a single bubble size given in Ref. [14], as the interval $\Delta\omega_o \rightarrow 0$ the neglected logarithmic term must be included, thus showing the approximation becomes less valid for very small bandwidths (small bubble size range).

The value of the terms in the bracket in Eq. (17a) are plotted in Fig. 2A for frequencies of 20, 50, and 100 kilocycles. The values of the damping constant are taken from Fig. 1A. The value of $\Delta\omega/\omega_o$ is 1/8, the small change in amplitude for each different frequency, and damping shows only a small dependence on damping.

The constant in Eq. (17a) may now be written

$$\frac{\alpha}{\omega_o^2} = \frac{8.68\ C_{ph}\rho\tau(r)}{4\pi\sqrt{2}\ \gamma P_a(\frac{g}{a})} \frac{\omega^2}{\omega_o^2} \left[F\left(\frac{\omega}{\omega_o}\right)\right] \tag{18a}$$

$$\frac{\alpha}{\omega_o^2} = \frac{8.68 \times 1 \times 1.48 \times 10^5\ \tau(r)}{4\pi\sqrt{2} \times 1.4 \times 10^6 P_a(\frac{g}{a})} \left[F\left(\frac{\omega}{\omega_o}\right)\right] = \frac{.0518\ \tau(r)}{P_a(\frac{g}{a})} \left[F\left(\frac{\omega}{\omega_o}\right)\right]$$

where P_a is now in atmospheres and $\frac{\omega^2}{\omega_o^2}$ is incorporated in the bracket term.

The last equation permits evaluation of the concentration, $\tau(r)$, in terms of the applied frequency characteristics, the inherent damping and the observed attenuation.

A P P E N D I X I I

CONVERSION OF DATA

APPENDIX II

CONVERSION OF DATA

The conversion of attenuation into concentration requires the formation of a sum as in Eq. (4a), Appendix I. This must, in some manner, be commensurate with the physical situation so as to approximate the form of the measured total attenuation pattern as a function of frequency. An example of this is Fig. 3A which was assembled from attenuation measurements taken in a typical water tunnel. As a first step to this end such a graph of total attenuation is broken down into a series of immediately adjacent parts on the frequency scale. Each of these parts is equivalent to one of the intervals (r_{n+1} to r_n) of Eq. (4a) where the bubble radius, r, has been converted to frequency.

The function I_n is given by Eq. (17a) where radii have been converted into frequency. The term $\frac{2\Delta\omega_o}{\omega_o}$ expresses the integral of integration (r_{n+1} to r_n) on the frequency scale. The value $\frac{\omega}{\omega_o} = 1$ is a convenient midband identification. An example of the division of the frequency scale of the measured data into a series of discrete bands is shown by the heavy vertical lines on Fig. 3A. Each line is located at $\frac{\omega}{\omega_o}$ equal to unity in its own interval and the lines are $2\frac{\Delta\omega}{\omega_o}$ apart. An arbitrary value of $1/8$ has been chosen for $\frac{\Delta\omega}{\omega_o}$; therefore the frequency value for each vertical line is $9/7$ times the frequency of the previous line. The $9/7$ value derives from $f_1 \times 9/8 = f_2 \times 7/8$.

The ordinate of Fig. 3A is plotted in units of $\frac{\alpha P_a (\frac{g}{a})}{30f^2}$ where the attenuation α is in db/cm and P_a is in psi; this mixed combination of units gives a convenient constant of 30.

The quantity

$$\frac{\omega^2}{\omega_o^2}\tan^{-1}\frac{2\eta\left(\frac{2\Delta\omega_o}{\omega_o}\right)\frac{\omega^2}{\omega_o^2}}{\left(1-\frac{\omega^2}{\omega_o^2}\right)^2+\eta^2\frac{\omega^2}{\omega_o^2}-2\left(\frac{\omega}{\omega_o^2}\right)^2\frac{\omega^2}{\omega_o^2}\left(\frac{\Delta\omega^2}{\omega_o^2}+1\right)}=F\left(\frac{\omega}{\omega_o}\right)$$

has been plotted in Fig. 2A for frequencies of 20, 50 and 100 kilocycles. Values of η were taken from the experimentally determined values as compiled by Turner [9], and as shown in Fig. 1A.

The value of the quantity $F(\frac{\omega}{\omega_o})$ when plotted on semi-logarithmic paper as in Fig. 2A may be used repeatedly like a template on succeeding determinations of concentration as will be described shortly.

On Fig. 3A the usual practice of plotting frequency on a logarithmic scale has been followed. The linear lengths on Fig. 3A should be chosen so as to equal the length of an equivalent ratio of $\frac{\omega}{\omega_o}$ on Fig. 2A. The length Z on Fig. 2A must equal the length Z on Fig. 3A.

From the basic nature of a logarithmic scale, that equal ratios cut off equal length at any position on the frequency scale, the templates of Fig. 3A may be superimposed at any point along the frequency scale of Fig. 3A. However, the variation of η with frequency will restrict this movement to small distances near the particular value of ω in $\frac{\omega}{\omega_o}$. When the first template from Fig. 2A is superimposed on the lowest frequency range (20 KC) of Fig. 3A, the tail of the template will contribute a value to the attenuation in the adjacent frequency interval. This must be subtracted before the next template is superimposed. In this case, the value is measured as A' on the bottom of the diagram and is subtracted at the top as shown on Fig. 3A. The next template is then superimposed with its ordinate suppressed by the value A' where $\frac{\omega}{\omega_o}=1$ (occurring at an interval $9/7 \times 20 = 25.8$ kilocycles) and so on until the complete graph is covered. In this progression templates are successively changed as η varies with frequency.

The loci of the peaks of the templates of Fig. 2A superimposed on Fig. 3A are the numbers related to the contribution of bubble concentration acting independently on the attenuation in that particular interval. Division by the peak value of $F(\frac{\omega}{\omega_o})$ in each interval and multiplication by the absolute width of the interval, $(2\Delta\omega_o)$, in cycles gives the total concentration of air in that interval. The frequency limits of each interval may now be converted into radii by Eq. (1).

Typical results of two such determinations in the St. Anthony Falls water tunnel are shown in Figs. 4A and 5A. The total time required to reduce an attenuation reading to concentration size distribution of this type requires about 35 minutes. This time could be reduced as familiarity with a particular situation is acquired. Many mechanical aids to the rapid plotting of data are available and could be utilized to much reduce the above time.

It can be noted on Fig. 1A that two experimenters have obtained much larger values of damping constants than most of the others. The significant difference between them is that the high value of η was obtained with swarms of bubbles while the lower values were obtained on single bubbles. As Fig. 2A and Eq. (17a) shows, the band width factor $\frac{\Delta\omega}{\omega_o}$ behaves like a damping factor dominating the amplitude while for a single bubble size η dominates the amplitude. Experimentally the only practical means of producing one bubble size is to use one bubble. Production of swarms of bubble invariably produce a range of sizes. It is possible then that these higher values of damping have included an effect of radii spread. In consequence the lower values of η, derived from single bubble experiments, currently appear most satisfactory for use in calculating Eq. (17a).

F I G U R E S

(1A through 5A)

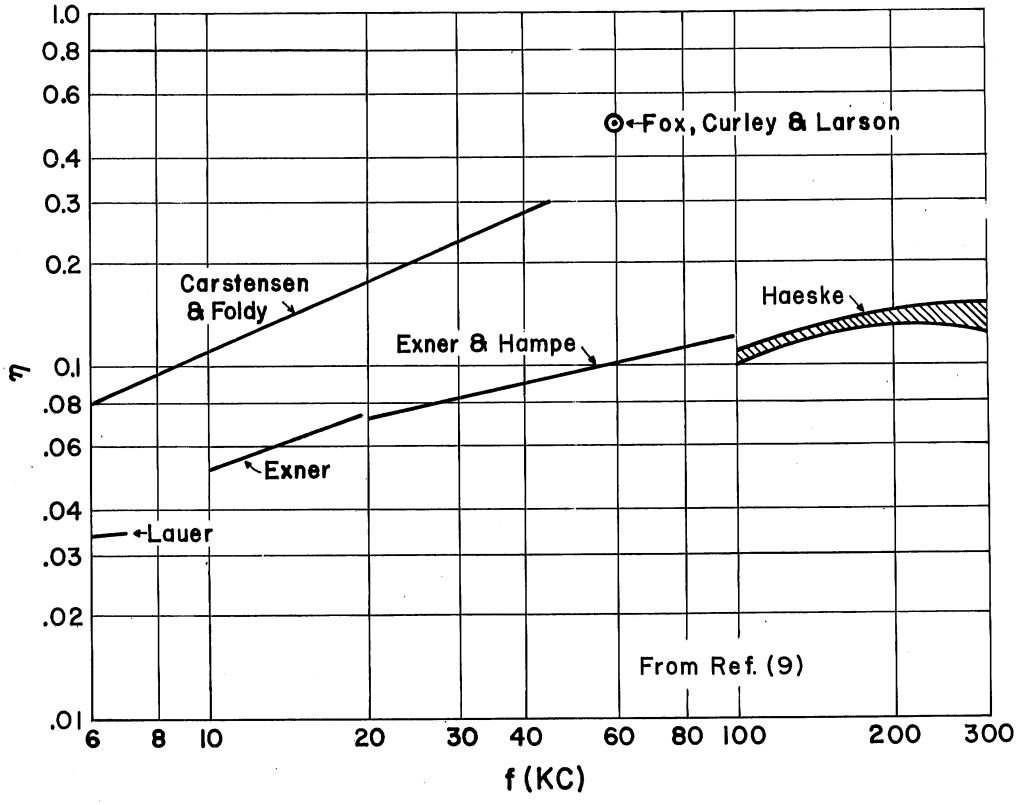

Fig. 1A - Damping Factor of Resonant Bubbles, Ref. [9]

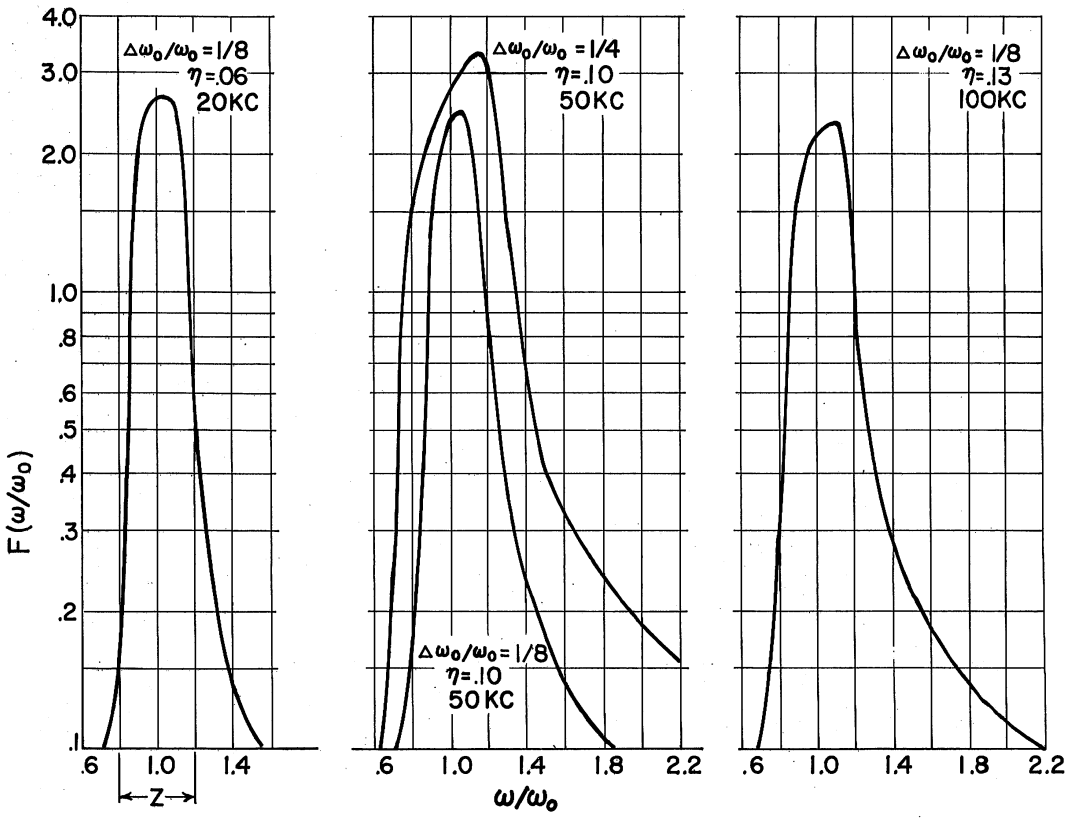

Fig. 2A - Attenuation Function Templates

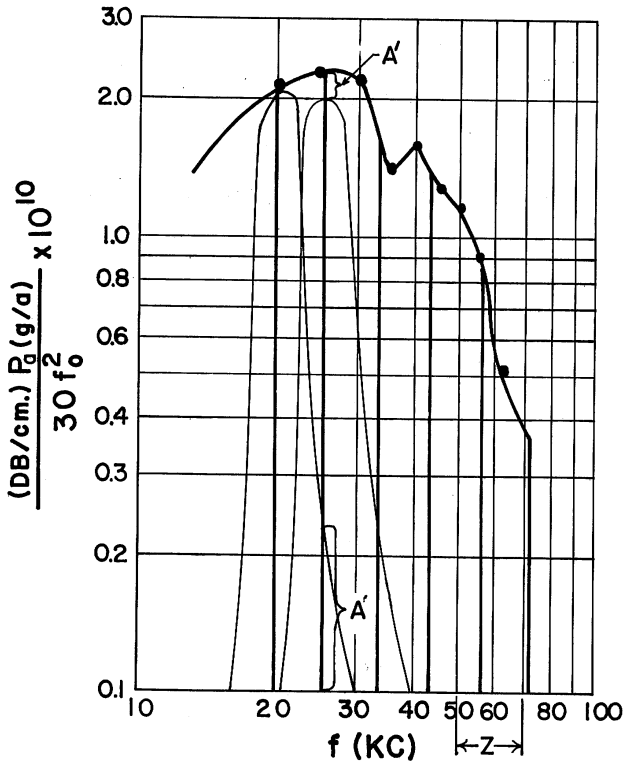

Fig. 3A - Plot of Experimental Data

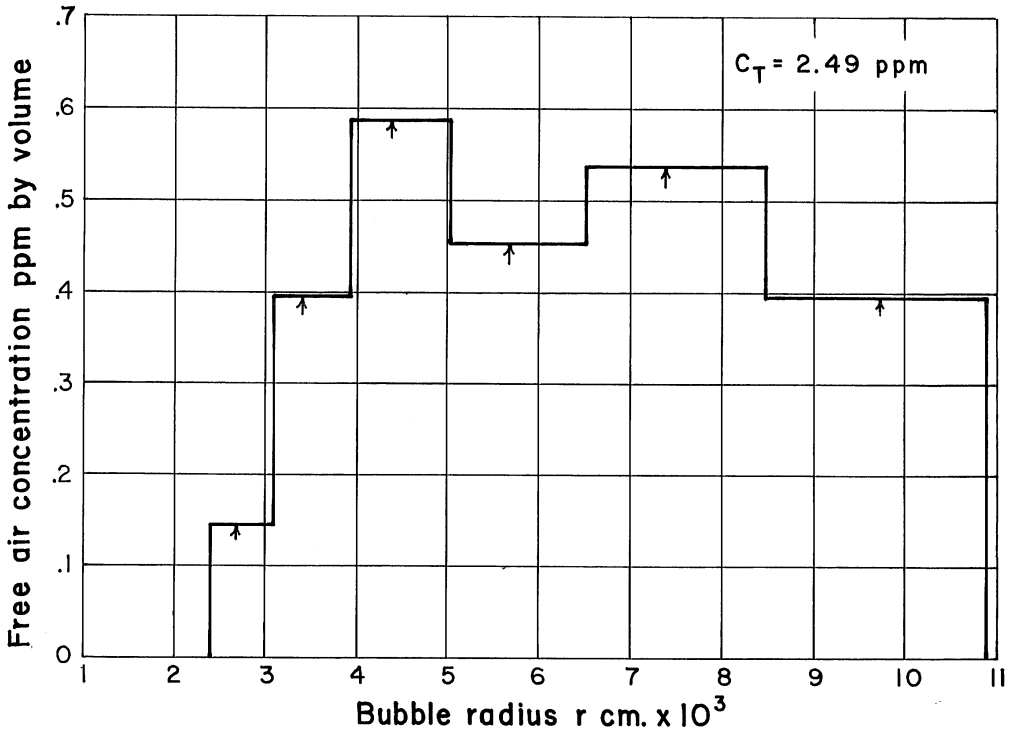

Fig. 4A - Typical Water Tunnel Bubble Distribution Values

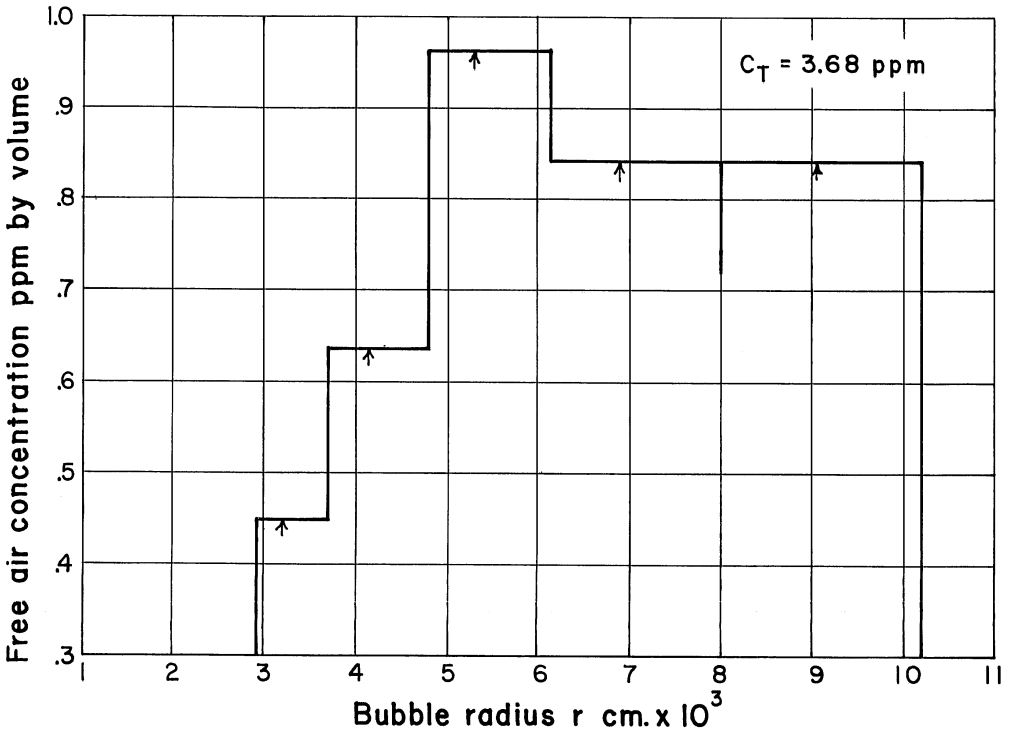

Fig. 5A - Typical Water Tunnel Bubble Distribution Values

DISTRIBUTION LIST FOR PROJECT REPORT NO. 70

of the St. Anthony Falls Hydraulic Laboratory

Copies	Organization
75	Commanding Officer and Director, David Taylor Model Basin, Washington 7, D. C., Attn: Code 513.
10	Chief, Bureau of Ships, Department of the Navy, Washington 25, D. C., Attn: Technical Library (Code 312). For distribution as follows: 5 - Technical Library 1 - Preliminary Design (Code 420) 1 - Hull Design (Code 440) 1 - Research and Division Planning (Code 320) 1 - Code 341B and 1 - Code 345
6	Chief, Bureau of Yards and Docks, Department of the Navy, Washington 25, D. C.
3	Chief, Bureau of Ordnance, Department of the Navy, Washington 25, D. C., Attn: Underwater Ordnance (Code Re6a).
3	Chief, Bureau of Aeronautics, Department of the Navy, Washington 25, D. C., Attn: Aero and Hydrodynamics (Code AD-3).
4	Chief of Naval Research, Department of the Navy, Washington 25, D. C. 3 - Mechanics Branch (Code ONR 438) 1 - Acoustic Branch (Code ONR 411)
1	Director, U. S. Naval Research Laboratory, Washington 25, D. C., Attn: Code 2021.
1	Commanding Officer, Office of Naval Research, Branch Office, 230 N. Michigan Avenue, Chicago 1, Illinois.
1	Commander, U. S. Naval Ordnance Laboratory, White Oak, Silver Spring, Maryland.
1	Commander, U. S. Naval Ordnance Test Section, 3202 East Foothill Boulevard, Pasadena, California.
1	Commanding Officer and Director, U. S. Navy Underwater Sound Laboratory, Fort Trumbull, New London, Connecticut.
2	Director, Ordnance Research Laboratory, Pennsylvania State University, University Park, Pennsylvania.
1	U. S. Naval Applied Science Laboratory, Naval Base, Brooklyn, N. Y. Attn: J. F. Lichtman.
1	Superintendent, U. S. Naval Postgraduate School, Monterey, California, Attn: Librarian.

Copies

1 Chief of Research and Development, Department of the Army, Washington 25, D. C.

1 Director, U. S. Waterways Experiment Station, Corps of Engineers, P. O. Box 631, Vicksburg, Mississippi.

1 Office of the Chief of Engineers, Department of the Army, Gravelly Point, Washington 25, D. C.

1 Director of Research National Aeronautics and Space Administration, 1724 F Street, N. W., Washington 25, D. C.

1 Director, Langley Aeronautical Laboratory, National Aeronautics and Space Administration, Langley Field, Virginia.

1 Director, Hydraulic Laboratory, Bureau of Reclamation, Denver Federal Center, Denver, Colorado.

1 National Aeronautics and Space Administration, Lewis Research Center, Cleveland, Ohio. Attn: Mr. R. S. Ruggeri.

10 Document Services Center, Armed Services Technical Information Agency Defense Documentation Center, Cameron Station, Alexandria, Virginia 22314.

2 Director, National Bureau of Standards, National Hydraulic Laboratory Washington 25, D. C.

2 Newport News Shipbuilding and Dry Dock Company, Newport News, Virginia. For distribution as follows:
1 - Senior Naval Architect
1 - Supervisor, Hydraulic Laboratory

2 California Institute of Technology, Division of Engineering, Pasadena 4, California.
1 - Dr. M. S. Plesset
1 - Dr. A. T. Ellis

2 Director, Davidson Laboratory, Stevens Institute of Technology, 711 Hudson Street, Hoboken, New Jersey.

1 Director, Hydraulic Laboratory, Worcester Polytechnic Institute, Worcester 2, Massachusetts.

1 Director, Hydrodynamics Laboratory, Massachusetts Institute of Technology, Cambridge 39, Massachusetts.

1 Head, Department of Naval Architecture and Marine Engineering, Massachusetts Institute of Technology, Cambridge 39, Massachusetts.

1 Director, Woods Hole Oceanographic Institute, Woods Hole, Massachusetts.

Copies

1 University of Michigan, Department of Nuclear Engineering, Ann Arbor, Michigan, Attn: Prof. F. G. Hammitt.

1 S. Logan Kerr and Co., P. O. Box 6, Flourtown, Pennsylvania, Attn: Mr. S. Logan Kerr.

1 Allis Chalmers Mfg. Co., Hydraulic Division, York, Pennsylvania, Attn: Mr. Wm. J. Rheingans.

1 Hydronautics, Incorporated, Pindell School Road, Howard County, Attn: Mr. Phillip Eisenberg.

1 Vitro Laboratories, 14000 Georgia Avenue, Silver Springs, Maryland, Attn: Mr. W. R. Turner.

1 Librarian, Engineering Societies Library, 29 West 39th Street, New York 18, New York.

2 Library, California Institute of Technology, Pasadena, California.

1 Librarian, Massachusetts Institute of Technology, Cambridge 39, Massachusetts.

1 Librarian, Library of Congress, Washington 25, D. C.

1 Librarian, School of Engineering, University of Texas, Austin, Texas.

3 Serials Division, University of Minnesota Library, Minneapolis, Minnesota.

1 Oceanics, Incorporated, Technical Industrial Park, Plainview, Long Island, New York, Attn: Dr. Paul Kaplan, President.

Project Report No. 70
St. Anthony Falls Hydraulic Laboratory

A WATER TUNNEL AIR CONTENT METER, by John M. Killen and John F. Ripken. February 1964. 41 pages incl. 17 illus. Contract Nonr 710(42).

This paper describes a system for measuring the size and concentration of free air bubble nuclei in the limited ranges of size and concentration thought to exist in a water tunnel. The system is based on measuring the amplitude attenuation of an acoustic pulse of sound as it is propagated across a water tunnel test section. An arbitrary method is proposed for converting the measured sound attenuation into size and concentration of air bubbles.

1. Nuclei (Cavitation)
2. Air Bubbles
3. Air Content
4. Cavitation
5. Water Tunnel

I. Title
II. Killen, John M.
III. Ripken, John F.
IV. St. Anthony Falls Hydraulic Laboratory
V. Contract No. 710(42)

Unclassified

Project Report No. 70
St. Anthony Falls Hydraulic Laboratory

A WATER TUNNEL AIR CONTENT METER, by John M. Killen and John F. Ripken. February 1964. 41 pages incl. 17 illus. Contract Nonr 710(42).

This paper describes a system for measuring the size and concentration of free air bubble nuclei in the limited ranges of size and concentration thought to exist in a water tunnel. The system is based on measuring the amplitude attenuation of an acoustic pulse of sound as it is propagated across a water tunnel test section. An arbitrary method is proposed for converting the measured sound attenuation into size and concentration of air bubbles.

1. Nuclei (Cavitation)
2. Air Bubbles
3. Air Content
4. Cavitation
5. Water Tunnel

I. Title
II. Killen, John M.
III. Ripken, John F.
IV. St. Anthony Falls Hydraulic Laboratory
V. Contract No. 710(42)

Unclassified

Project Report No. 70
St. Anthony Falls Hydraulic Laboratory

A WATER TUNNEL AIR CONTENT METER, by John M. Killen and John F. Ripken. February 1964. 41 pages incl. 17 illus. Contract Nonr 710(42).

This paper describes a system for measuring the size and concentration of free air bubble nuclei in the limited ranges of size and concentration thought to exist in a water tunnel. The system is based on measuring the amplitude attenuation of an acoustic pulse of sound as it is propagated across a water tunnel test section. An arbitrary method is proposed for converting the measured sound attenuation into size and concentration of air bubbles.

1. Nuclei (Cavitation)
2. Air Bubbles
3. Air Content
4. Cavitation
5. Water Tunnel

I. Title
II. Killen, John M.
III. Ripken, John F.
IV. St. Anthony Falls Hydraulic Laboratory
V. Contract No. 710(42)

Unclassified

Project Report No. 70
St. Anthony Falls Hydraulic Laboratory

A WATER TUNNEL AIR CONTENT METER, by John M. Killen and John F. Ripken. February 1964. 41 pages incl. 17 illus. Contract Nonr 710(42).

This paper describes a system for measuring the size and concentration of free air bubble nuclei in the limited ranges of size and concentration thought to exist in a water tunnel. The system is based on measuring the amplitude attenuation of an acoustic pulse of sound as it is propagated across a water tunnel test section. An arbitrary method is proposed for converting the measured sound attenuation into size and concentration of air bubbles.

1. Nuclei (Cavitation)
2. Air Bubbles
3. Air Content
4. Cavitation
5. Water Tunnel

I. Title
II. Killen, John M.
III. Ripken, John F.
IV. St. Anthony Falls Hydraulic Laboratory
V. Contract No. 710(42)

Unclassified